Biotechnology Journal
www.biotechnology-journal.com

Biotechnol. J. 2014, 9, 192–202

DOI 10.1002/biot.201300202

Review

# Decoding spatial and temporal features of neuronal cAMP/PKA signaling with FRET biosensors

*Liliana R. V. Castro[1,2], Elvire Guiot[1,2], Marina Polito[1,2], Danièle Paupardin-Tritsch[1,2] and Pierre Vincent[1,2,*]*

[1] CNRS UMR7102, Paris, France
[2] Sorbonne Universités, UPMC Univ Paris 06, UMR7102, Paris, France

Cyclic adenosine monophosphate (cAMP) and the cyclic-AMP-dependent protein kinase (PKA) regulate a plethora of cellular functions in virtually all eukaryotic cells. In neurons, the cAMP/PKA signaling cascade controls a number of biological properties such as axonal growth, pathfinding, efficacy of synaptic transmission, regulation of excitability, or long term changes. Genetically encoded optical biosensors for cAMP or PKA are considerably improving our understanding of these processes by providing a real-time measurement in living neurons. In this review, we describe the recent progress made in the creation of biosensors for cAMP or PKA activity. These biosensors revealed profound differences in the amplitude of the cAMP signal evoked by neuromodulators between various neuronal preparations. These responses can be resolved at the level of individual neurons, also revealing differences related to the neuronal type. At the sub-cellular level, biosensors reported different signal dynamics in domains like dendrites, cell body, nucleus, and axon. Combining this imaging approach with pharmacology or genetic models points at phosphodiesterases and phosphatases as critical regulatory proteins. Biosensor imaging will certainly emerge as a forefront tool to decipher the subtle mechanics of intracellular signaling. This will certainly help us to understand the mechanism of action of current drugs and foster the development of novel molecules for neuropsychiatric diseases.

Received 01 JUL 2013
Revised 02 DEC 2013
Accepted 08 JAN 2014

**Keywords:** Biosensor · Cyclic AMP · Live-cell imaging · Neurons · Protein kinase A

## 1 Introduction

The cyclic adenosine monophosphate (cAMP) and protein kinase A (PKA) signaling pathway is involved in virtually all physiological processes. A number of G-protein coupled receptors control cAMP production via stimulatory (Gs) or inhibitory (Gi) G-proteins, respectively. These G-proteins modulate the activity of adenylyl cyclase (AC), a transmembrane enzyme, which produces cAMP. cAMP affects various downstream effectors, including cyclic nucleotide gated (CNG) channels [1], cationic channels activated by hyperpolarization of the $I_h$ family [2], exchange protein directly activated by cAMP (Epac) [3], and cAMP-dependent PKA [4, 5].

The cAMP/PKA signal, like many other cellular signals, should be understood in the multiple dimensions of the living cell. The temporal dimension is obviously a critical one, as the PKA signal rises following a stimulus and then declines over time as the stimulus is removed and/or feedback mechanisms revert the signal to baseline. The spatial dimension also plays a role since the concentration of signaling molecules decreases with distance: cAMP diffuses into the cytosolic volume and is degraded by

**Correspondence:** Dr. Pierre Vincent, Team "Cellular Integration of Neuromodulatory Processes," UMR8256 CNRS UPMC, 9, quai St Bernard, F-75005 Paris, France
E-mail: pierre.vincent@upmc.fr

**Abbreviations: AC**, adenylyl cyclases; **AKAP**, A kinase anchoring proteins; **AKAR**, A-kinase activity reporter; **cAMP**, cyclic adenosine monophosphate; **CFP**, cyan fluorescent protein; **CNG**, cyclic nucleotide gated channel; **Epac**, exchange protein directly activated by cAMP; **Epac1-camps**, Epac1-based cAMP sensor; **Epac2-camps**, Epac2-based cAMP sensor; **FlCRhR**, fluorescein-labeled catalytic subunit and rhodamine-labeled regulatory subunit; **FRET**, Förster resonance energy transfer; **HCN**, hyperpolarization-activated cyclic nucleotide-modulated channel; **PDE**, phosphodiesterase; **PKA**, cAMP-dependent protein kinase; **$^{T}$Epac$^{VV}$**, Epac-based sensor with Turquoise, Venus and cpVenus; **YFP**, yellow fluorescent protein

phosphodiesterases (PDE), processes classically modeled with reaction-diffusion equations. Protein–protein interactions, like those mediated by A kinase anchoring proteins (AKAPs) or proteins interacting with membrane receptors, maintain all partners of the signaling cascade in close proximity in signaling microdomains [6–8]. In addition to these factors, the geometry of the cell can affect signal integration, with a high surface-to-volume ratio favoring the accumulation of cAMP and the activation of PKA in thin dendrites versus the cell body [9]. Temporal and spatial features of intracellular signal integration are critical in the particular case of neurons: these cells exhibit complex morphological domains such as dendritic tree, spines, cell body, and axon, each endowed with specific functions. Biosensor imaging is therefore highly needed to help understand the fundamental mechanisms involved in signal integration in neurosciences.

The last decade has seen the development of biosensor imaging to monitor specific intracellular events [10, 11]. A number of such sensors were created for various biological signals, some of these being designed more specifically for applications in neurosciences, like genetically encoded calcium or voltage indicators [12, 13] or glutamate indicators [14–17]. In this rapidly growing field, this review focuses specifically on the cAMP/PKA signaling cascade in neurons, although many aspects could be transposed to other signaling cascades.

## 2 FRET-based sensors to detect cAMP or PKA signals

The use of biochemical approaches such as radioimmunoassay allows for the quantification of total cAMP concentrations or kinase activities in cell and tissue homogenates. Although very specific and sensitive, these biochemical methods require large amounts of cells or tissue, which strongly reduces the temporal resolution and precludes specific analysis in sub-cellular microdomains. Ion channels sensitive to cyclic nucleotides such as the CNG channels and the hyperpolarization-activated cyclic nucleotide-modulated channels (HCN) [1] provide a way to monitor changes in cAMP concentration using electrophysiological recordings. CNG channels have been further engineered to improve channel properties [18], and this approach demonstrated the sub-membrane compartmentation of the cAMP signal [19]. The use of such channels is however difficult in neurons where their expression would likely perturb excitability and calcium fluxes. The development of FRET biosensors overcome many of these limitations by allowing the visualization of cAMP/PKA signaling in individual cells with high temporal and spatial resolution.

Many FRET-based biosensors are constituted of a domain sensitive to the biological signal of interest inserted between two fluorophores, the donor and the acceptor. Förster resonance energy transfer (FRET) is a physical process whereby the energy of an excited fluorophore (the donor) is transferred by resonance to a neighboring fluorophore (the acceptor), a phenomenon that strongly depends on the relative distance and/or orientation between the donor and acceptor [20, 21]. The biological signal triggers a conformational change of the sensor moiety, which modifies the extent of FRET from donor to acceptor upon donor excitation, leading to reciprocal changes in fluorescence intensities at the wavelength of donor and acceptor. A number of FRET biosensors have been devised in the last decade [11, 22] and we will focus here on biosensors specifically developed to monitor cAMP levels and PKA-mediated phosphorylation events with their applications in neurobiology.

The first cAMP sensor used recombinant PKA with the catalytic subunit labeled with fluorescein (donor) and the regulatory subunit labeled with rhodamine (acceptor): the dissociation of the regulatory and catalytic subunit upon cAMP binding was monitored as a decrease in FRET between the two fluorophores [23]. This biosensor called FlCRhR was used in invertebrate neurons [24, 25] and embryonic spinal neurons [26]. However, this first biochemical sensor remained impractical to use in vertebrate neurons because the recombinant and labeled holoenzyme had to be injected into living cell, which proved to be a difficult task [27, 28].

The first genetically encoded indicator for cAMP used the same design as FlCRhR, first replacing the chemical fluorophores fluorescein and rhodamine with the GFP and BFP fluorophores, and later on with CFP and YFP [29, 30]. This sensor reports the dissociation of the regulatory and catalytic subunits of PKA by a decrease in FRET between these fluorophores. This sensor can be localized in different subcellular domains to AKAPs [31, 32]. This type of sensor needs equal expression of both subunits to form the holoenzyme in the transfected cell and excess of either subunit can complicate signal analysis. Moreover, this sensor still has a kinase activity and its expression in neurons will likely interfere with the cAMP/PKA signaling cascade. Genetically encoded single chain FRET biosensors devoid of catalytic activity were developed using the cAMP-binding domain B of RIIβ subunit of PKA as cAMP sensing domain (PKA-camps sensor) [33]. In parallel, other sensors were developed using either the whole Epac protein or truncated forms harboring its cAMP-binding domain [33–35]. For example Nikolaev and coworkers developed a cAMP sensor composed of a single cAMP binding domain of either Epac1 or Epac2, fused to CFP and YFP to generate Epac1-camps and Epac2-camps sensors, respectively [33]. Epac2-camps exhibits a slightly higher cAMP sensitivity than Epac1-camps (0.9 μM vs. 2.4 μM) and both exhibit significantly faster kinetics than the sensor based on PKA holoenzyme. A transgenic mouse line was then created with ubiquitous expression of the Epac1-camps sensor (CAG-Epac1-camps), allow-

ing the study of the cAMP signaling in more physiological conditions [36]. Epac2-camps was further modified by mutating the cAMP-binding domain to increase its sensitivity to cAMP. This sensor, called Epac2-camps300 [37] has an $EC_{50}$ for cAMP of 0.3 μM and is suitable for measurements of the very low cAMP levels present in mature neurons [38] (see below). Another cAMP sensor was derived from the cAMP-binding domain of the hyperpolarization-activated cationic channel HCN2 [39]. This sensor called HCN2-camps, has a fairly low cAMP sensitivity with an $EC_{50}$ of 6 μM.

While most biosensors use the traditional CFP/YFP pair of fluorophores, or their close derivatives, it may be needed to perform recordings at other wavelength and various versions of Epac-based sensors have been created with GFP donor and various yellow and red acceptors [40, 41]. Some limitations of biosensor imaging include sensitivity to photobleaching, pH, and temperature, and it is therefore desirable to use the brightest as well as the most stable fluorophores in biosensor constructs. Thus, taking advantage of the CFP-derived donor fluorophore Turquoise and using the Epac1 backbone, $^{T}Epac^{VV}$ showed improved photostability and outstanding ratio changes upon cAMP activation [42]. This sensor was further improved by replacing the donor with mTurquoise2 and the acceptor pair with a single cp174Citrine. Its sensitivity for cAMP was increased by introducing the Q270E mutation in the cAMP-binding domain, yielding $Epac-S^{H150}$ [43].

One step downstream, the effects of cAMP on PKA activity can be investigated using the A-kinase activity reporter (AKAR). This is a family of FRET biosensors composed of CFP as FRET donor, a phosphoamino acid binding domain, a PKA-specific substrate, and YFP as FRET acceptor: when this protein is phosphorylated by PKA, the phosphoamino acid binding domain binds onto the phosphorylated PKA substrate, driving a conformational change, which increases FRET between CFP and YFP. After the initial proof of concept of AKAR1, which lacked reversibility [44], AKAR2 [45] was a well-usable reporter, rapidly superseded by AKAR3, where the acceptor was changed for a circularly permuted citrine [46]. Changing the CFP donor for the brighter Cerulean yielded AKAR4 [47] while Aquamarine led to $^{Aq}AKAR^{Cit}$ with improved photostability [48].

Although commonly dubbed "PKA sensors," one must keep in mind that the phosphorylation level of the biosensor results from the equilibrium between PKA-dependent phosphorylation and dephosphorylation performed by phosphatases, and is therefore a reporter of the phosphorylation level of a PKA substrate.

A similar strategy was followed to monitor the phosphorylation level of CREB, a critical transcription factor. CREB is phosphorylated by PKA, as well as by the calcium/calmodulin-dependent kinase IV and MAP kinases. This biosensor, called ICAP, reported CREB activation after direct activation of the cAMP pathway by forskolin, as well as in response to depolarization or activation of MAP kinase [49].

## 3 Amplitude of the cAMP/PKA signal

### 3.1 Striking differences in cAMP levels in different neuronal settings

Strong cAMP responses to β-adrenergic stimulation were recorded with Epac1-camps in various cell types like macrophages, cardiomyocytes, and fibroblasts [36, 50]. Cell lines also exhibited strong responses such as the MIN6 pancreatic cell line, which strongly responds to glucose [51], or HEK-293 cell line, which responded to the activation of β2-adrenergic receptors [52]. In neurons, spontaneous cAMP oscillations were reported in cultured retinal ganglion cells with a low-sensitivity cAMP sensor [53] and cAMP responses were recorded with Epac1-camps after β-adrenergic stimulation in primary cultures of hippocampal neurons [9, 33, 36] or after ATP stimulation in organotypic cultures of brain-stem slices [54].

In contrast to these measurements, the bulk cytosol of pyramidal neurons in brain slice preparations showed no or little response with cAMP biosensors when various Gs-coupled receptors were activated: monoamine receptors (β1-adrenergic and dopamine $D_1$) as well as receptors to neuropeptides (vasoactive intestinal peptide, corticotropin-releasing factor or pituitary adenylate cyclase-activating peptide) all failed to activate Epac1-camps, a probe with an $EC_{50}$ for cAMP of 2.4 μM [38, 55, 56]. However, when β1-adrenergic or dopamine $D_1$ receptor agonists were tested with the more sensitive Epac2-camps300 sensor, clear positive responses were obtained [38, 56]. At the level of PKA, activation of these various receptors produced responses ranging from 20 to 80% of the maximal response (Fig. 1A), showing that although activation of these receptors produce little cAMP, they nonetheless all succeed in activating PKA in the cytosol. This observation was further investigated for the $D_1$ dopamine receptor in pyramidal cortical neurons: for a same full activation of the $D_1$ receptor, three biosensors exhibited responses of increasing amplitudes, consistent with an increasing sensitivity of these biosensors: Epac1-camps<Epac2-camps300<AKAR3 (Fig. 1B, left) [56].

Overall, these data show that the activation of various Gs-coupled receptors in pyramidal cortical neurons trigger responses at the cAMP level that remain in the submicromolar range, though sufficient to activate PKA. Modeling studies suggested that free cAMP concentration is about 250 nM in the soma during β1-adrenergic stimulation, and this fairly low cAMP concentration results from a strong phosphodiesterase activities [9], with type 4 phosphodiesterase (PDE4) being one of the main phosphodiesterase activities in these neurons [38].

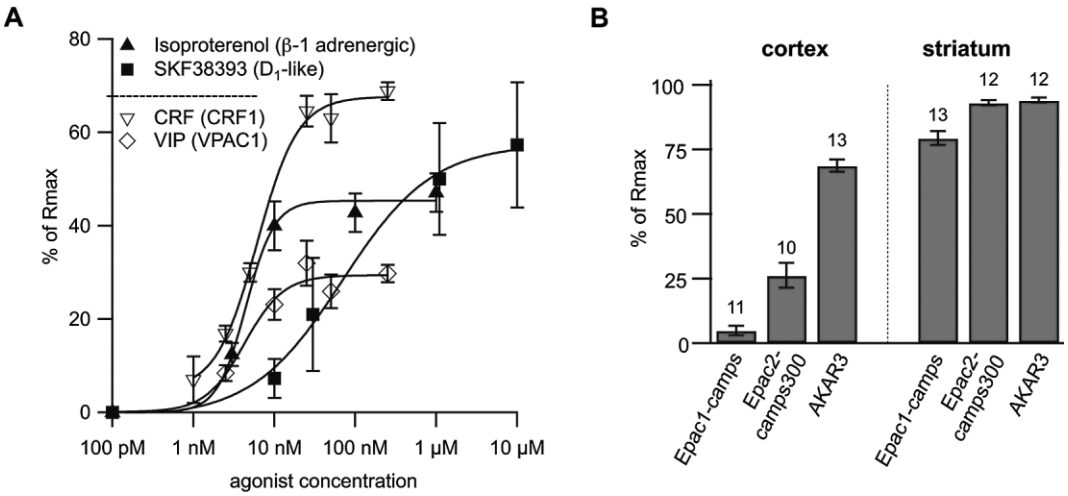


**Figure 1.** Biosensors quantitatively report responses to neuromodulatory activation. (**A**) Activation of different Gs-coupled receptors produces PKA responses of different amplitudes. β-1 adrenergic, $D_1$ dopamine, CRF1, and VPAC1 receptor were respectively activated by application of the β adrenergic agonist isoproterenol, the dopamine $D_1$ agonist SKF38393 and the neuropeptides CRF (corticotropin-releasing factor) and VIP (vasoactive intestinal peptide). PKA activity was measured on pyramidal neurons of the cortex expressing the AKAR2 or AKAR3 sensors. Data present the mean response as a percentage of the maximal response ($R_{max}$, see text for explanations); error bars indicate SEM; each data point was obtained from 3 to 15 independent experiments. Data compiled from [38, 55, 56]. (**B**) In response to a same dopaminergic stimulation, cortical neurons show much lower cAMP/PKA responses than striatal neurons. $D_1$ receptors were stimulated with a saturating dose of SKF38393 (1 µM); the cAMP responses were measured with the biosensors Epac1-camps and Epac2-camps300; the PKA responses were measured with AKAR3. The response amplitude measured with each biosensor was normalized with respect to the maximal biosensor response ($R_{max}$) and plotted as a histogram. Error bars indicate the SEM; the number of independent experiment is indicated above each bar. The difference between cortex and striatum was significant for each of the three biosensors ($p<10^{-8}$ unpaired two-tailed t-test). Figure 1B is from [56].

The low cAMP level in mature neurons in brain slice preparations contrasts with the high level recorded in cultured embryonic neurons, suggesting that the cAMP level may depend on the developmental stage: undifferentiated neurons may need high cAMP to grow and setup their connections [57], a process that may be related to the expression of other adenylyl cyclases such as AC8 in embryonic neurons, and that is needed for proper axonal and dendritic differentiation [58]. Later on, once the connections are established, maintaining high cAMP responses may be unnecessarily "expensive" for the neuron, while maintaining a low global cAMP level is needed to establish a sub-cellular compartmentation of cAMP responses. Thus, PDE4 is critical to maintain this sub-cellular compartmentation in pyramidal neurons where high cAMP levels are restricted underneath the membrane [38].

This model however does not apply to all brain regions: compared to pyramidal cortical neurons, striatal spiny neurons responded to dopamine $D_1$ receptor activation with particularly large cAMP levels, reaching a level close to the maximum with all three biosensors tested (Fig. 1B, right) [56]. A number of biochemical specificities of striatal neurons, like a lack of PDE4 activity, a powerful adenylyl cyclase activity, and a positive feed-back mechanism mediated at the level of phosphatases suggest that these neurons are specifically geared to produce high cAMP levels. We hypothesize that this feature is related to the function of these neurons, which detect the very brief dopamine signals associated with reward.

### 3.2 Calibration of the ratio response, and its limitations

Theoretically, the optical response of a dual wavelength (ratiometric) sensor can be calibrated to convert the ratio value into an absolute ligand concentration. This was initially established for chemical calcium dyes [59] and the same equations apply to cAMP sensors [52, 54, 60]. This calibration uses the $EC_{50}$ and Hill coefficients, determined in vitro for most published cAMP sensors. In addition, the conversion of ratio measurements into cAMP concentrations requires the determination of $R_{min}$ and $R_{max}$, which are the ratio values in the absence and in the presence of saturating concentrations of cAMP, respectively. $R_{max}$ is obtained by maximally stimulating adenylyl cyclase with forskolin together with inhibiting PDE with IBMX, or using a membrane permeant cAMP analog like 8-Br-2′-O-Me-cAMP-AM; $R_{min}$ may be obtained by inhibiting adenylyl cyclases with dideoxy-adenosine, SQ22536 or MDL-12330A [54, 56, 60]. As there is some cell-to-cell variability in these values, the calibration must be applied for every individual cell.

Such conversion of ratio measurements into absolute concentrations may not be required to interpret the data:

as long as the baseline ratio is close to $R_{min}$, biological responses can be quantified as a percentage of $R_{max}$ [38, 56] and comparisons using biosensors with different sensitivities provided a clear picture of the cAMP levels present in the cytosol of cortical and striatal neurons (see above). The Epac1-camps, Epac2-camps and $^{T}Epac^{VV}$ sensors for cAMP have an $EC_{50}$ for cAMP from 1 to 15 μM, while the Epac2-camps300 sensor was mutated to lower its $EC_{50}$ down to 0.3 μM [37], thus covering a fairly large concentration range. In addition, PKA sensors of the AKAR type have the highest sensitivity, as minute amounts of cAMP are sufficient to activate PKA, which can phosphorylate a number of biosensor molecules.

### 3.3 The biosensor buffers the response to be measured

Biosensor concentration may further complicate the interpretation of ratio measurements: if biosensor molecules are present in large excess compared to cAMP, only a small fraction of the biosensor will be activated and the ratio will report a lower cAMP concentration than what would have occurred in the absence of the biosensor. Excessive biosensor concentration, by buffering cAMP, also prevents cAMP from acting on its physiological targets. The lowest biosensor concentration sufficient for a measurement is in the sub-micromolar range, a concentration that should not affect the biological signal. However, biosensor concentrations of several tens of micromolar can be reached easily [61, 62], where it certainly impacts the concentration measurement. While determining accurately the concentration of a biosensor inside a living cell is technically delicate, it is quite easy to verify the impact of biosensor concentration on the cAMP responses by plotting the amplitude of the cAMP response versus the biosensor fluorescence level: low fluorescence intensity, indicative of low biosensor expression level, should be associated with responses of larger amplitude whereas high fluorescence intensities, indicative of large biosensor concentrations, potentially associated with a buffering effect, should be associated with ratio responses of smaller amplitude. This negative trend was not observed in pyramidal cortical neurons showing that a buffering effect did not affect the responses in these precise conditions [56].

## 4 Spatial analysis of the cAMP/PKA signal

Biosensor imaging provide data in the spatial dimension with the characteristic resolution of optical microscopy, which allow for the monitoring of individual neurons as well as recording from specific sub-cellular domains.

### 4.1 Monitoring cAMP/PKA responses in distinct individual neurons

Analysis of the cAMP response with Epac1-camps in individual neurons in the Drosophila brain revealed specific sub-populations of neurons that responded differently to the PDF neuropeptide [63, 64]. Selective measurement at the level of individual neurons was also critical in the striatum. Medium spiny neurons (MSNs) constitute 95% of the neuronal population in the striatum: approximately half MSNs express dopamine $D_1$ receptors and belong to the anatomical "direct pathway," while the other half express dopamine $D_2$ receptors together with adenosine $A_{2A}$ receptors and belong to the "indirect pathway" [65, 66]. $D_1$ dopamine and $A_{2A}$ adenosine receptors are positively coupled to the intracellular signaling cascade of cAMP/PKA, while $D_2$ dopamine receptors are negatively coupled to cAMP/PKA. Biosensor imaging with two-photon microscopy clearly showed this dichotomy as half of the neurons responded positively to the activation of dopamine $D_1$ receptors while the other half responded to the stimulation of adenosine $A_{2A}$ receptors (Fig. 2A) [56]. This approach thus allows for the specific analysis of cAMP/PKA responses in functionally identified individual neurons within the anatomically intact context of a brain slice.

### 4.2 cAMP/PKA signals in sub-cellular domains

At a smaller spatial scale, biosensor imaging with two-photon microscopy also revealed how different domains of the neuronal cell (dendrites, cell body, and different axon terminals) exhibit specificities in their neuromodulatory responses. In Drosophila, biosensor imaging revealed different responses to dopamine, octopamine, or forskolin in different cellular domains and demonstrated the importance of PDE in maintaining sub-cellular compartmentation of the cAMP signal [67, 68]. In mammalian neurons, sub-cellular differences were also reported by two-photon microscopy: thin dendrites revealed larger responses to β-adrenergic stimulation or phosphodiesterase inhibition in thin remote dendrites than in the cell body (Fig. 2B), consistent with confined space accumulating cAMP more easily than the large somatic volume [38]. Although this had been predicted theoretically and verified in cultured neurons [9], brain slice imaging provided a clear experimental confirmation of the importance of cell geometry on signal integration in morphologically intact neurons.

cAMP/PKA signals at the membrane are particularly important in neurons since a number of ion channels are regulated either by direct binding of cAMP or via PKA-mediated phosphorylation. Electrophysiological recordings thus allow real-time monitoring of PKA activity on membrane channels and, interestingly, provide data consistent with biosensor recordings in thin dendritic

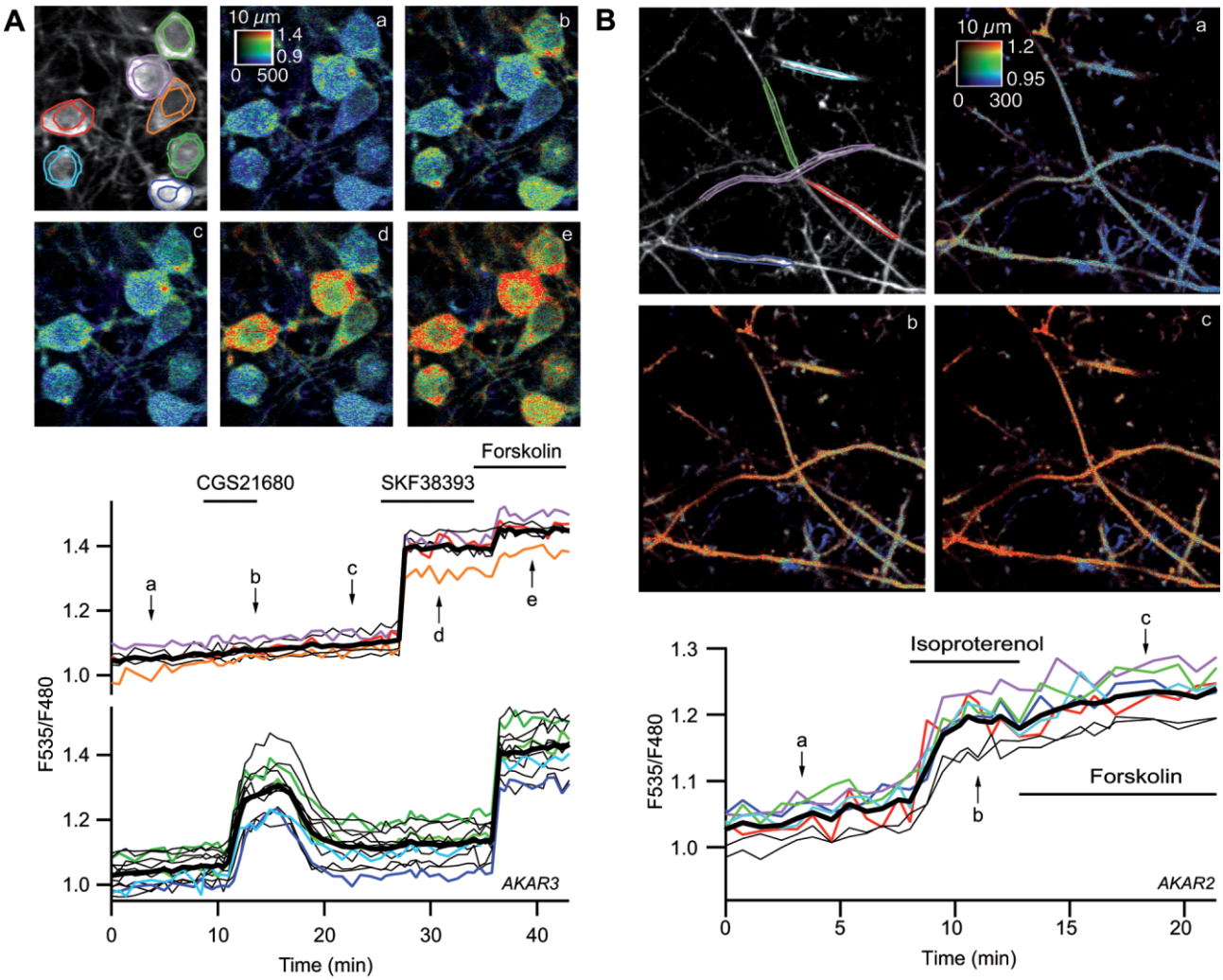


**Figure 2.** Two-photon imaging of a PKA-sensitive biosensor expressed in mouse brain slice provides selective measurements in individual neurons and in thin dendrites. (**A**) Imaging PKA activation with AKAR3 in medium spiny neurons of the striatum reveals two distinct neuronal populations, which respond selectively to the activation of either adenosine $A_{2A}$ receptor (with CGS21680) or dopamine $D_1$ receptor (with SKF38393). Traces are separated into two plots on the basis of their response to the $A_{2A}$ agonist or the $D_1$ agonist. The figure is from [56]. (**B**) Biosensor imaging reports large, almost saturating PKA responses to β-adrenergic stimulation in thin remote dendrites of cortical neurons expressing the AKAR2 sensor. The figure is from [79], with kind permission from Springer Science and Business Media. (A, B) Gray scale images show the raw fluorescence at 535 nm. Pseudocolor images represent the F535/F480 emission ratio at the times indicated by the corresponding arrows on the graph below. The calibration squares indicate fluorescence intensity horizontally and F535/F480 ratio vertically. Each trace on the graphs indicates the F535/F480 emission ratio measurements on the regions indicated by the color contour on the gray-scale image; thin traces in black correspond to cells outside the displayed region; the thick black line represents the average of all the traces. SKF38393 (1 μM), CGS21680 (1 μM), isoproterenol (1 μM) and forskolin (13 μM) were added in the bath during the time represented by the horizontal bar.

branches, where the biosensor reports mainly sub-membrane cAMP/PKA signals [38]. Similar sub-membrane compartmentation of the cAMP signal was reported in PC12 cells using an AKAR sensor targeted to the membrane with a K-Ras domain [69].

Further analysis of the sub-cellular compartmentation of the cAMP/PKA signal can be obtained using targeting sequences to address the biosensor into other sub-cellular domains of interest. The PKA response was monitored in intralaminar thalamic neurons which showed that the PKA response progresses temporally, starting at the membrane, where events occur on the time scale of tens of seconds as reported by electrophysiological recordings, then progresses into the cytosol where responses take place over a few minutes, and later access the nucleus after more than 10 min (Fig. 3) [70]. While direct imaging of signaling microdomains may be beyond the spatial resolution of optical microscope, it remains however possible to target the biosensor to these signaling microdomains using specific peptidic sequences and measure the aver-

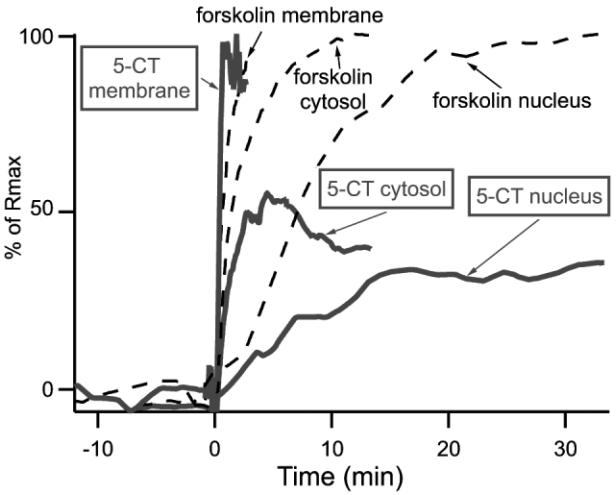


**Figure 3.** Kinetics of PKA responses at the membrane, in the cytosol, and in the nucleus in intralaminar thalamic neurons. PKA activation at the membrane was measured with patch-clamp recordings by monitoring a PKA-sensitive potassium current. PKA activation in the cytosol and the nucleus was measured by ratiometric imaging using respectively the AKAR2 and AKAR2-NLS sensors. The thick trace represents the responses to 100 nM 5-carboxamidotryptamine (5-CT), an agonist of serotonin 5-$HT_7$ receptor. Dotted lines are responses to 13 µM forskolin, used to normalize the amplitude for the cytosol and nucleus. The figure is from [70].

age biosensor signal over a number of such signaling domains. This was done in various non-neuronal cells [44, 46, 71] but so far not applied to neuronal preparations. This task may end-up being more difficult than it seems as a number of artifacts can result from expressing large amounts of targeted biosensors, ranging from environmental effects on the biosensor signal to disruption of the signaling microdomains by the biosensor itself. Alternatively, biosensor imaging may become very handy to analyze the impact of signaling microdomain disruption on intracellular signal propagation: AKAP disruption with Ht31 peptide or shRNA strongly reduced the efficacy of the cAMP signal on CREB phosphorylation, as reported by the ICAP biosensor [49].

## 5 Dynamics of the cAMP/PKA signals

The temporal dimension is a critical aspect of neural encoding in the brain and the dynamics of cAMP/PKA signaling is intimately related to neuronal function. Genetically encoded indicators open new possibilities for the analysis of the dynamics of the cAMP/PKA signaling in neurons, provided that biosensors have sufficient intrinsic temporal resolution. While the PKA-based sensors showed a complex temporal response, Epac-based sensors responded to cAMP within less than a few seconds [33, 53]. PKA sensors of the AKAR family also respond rapidly to brief stimuli as shown by the immediate response to cAMP uncaging in cardiac myocytes and in thalamic neurons [70, 72]. Biosensor imaging in neuronal preparations revealed the time-course of cAMP/PKA signals: in intralaminar thalamic neurons, the response to bath application of forskolin increased AKAR2 ratio immediately upon application of the drug, and reached its maximum in ~6 min [70]. Faster responses to forskolin were observed in pyramidal neurons of the prefrontal cortex (60 s) [56], in medium-spiny neurons of the striatum (25 s) [43, 56] and in retinal ganglion cells (20 s) [53].

The importance of temporal integration was illustrated recently in a study, which demonstrated that striatal neurons have a specific ability to decode sub-second dopamine signals [56]. Phasic dopamine signals were mimicked by releasing caged-dopamine (5 µM) with a flash of UV light for various duration (0.1, 0.3, and 1 s) while monitoring PKA activity with AKAR3 (Fig. 4). For both cortex and striatum, dopamine uncaging resulted in a transient increase in AKAR3 emission ratio. However, the overall responses differed considerably between the two brain regions: cortical neurons generated no response or a small-amplitude responses, whereas striatal neurons displayed an almost maximal response. Importantly, only striatal neurons showed an increase in cFos expression after brief dopamine stimulation, showing that the difference in response dynamics affects the physiological response. Such differences were shown to be related to differential expression of signaling proteins like PDE and DARPP-32, which determine the integrative properties of each neuron [56].

Simultaneous imaging of calcium and cAMP/PKA signals gave new insights on the interactions between these two signaling cascades in various non-neuronal cell types [51, 73, 74]. The same quantitative approach applied to spontaneously active neurons showed the interactions between periodic calcium and cAMP transients. This was illustrated in developing spinal cord neurons where a calcium signal triggered transient increases in cAMP, and reciprocally, cAMP levels regulated the frequency of calcium transients [26]. In retinal ganglion cells, the calcium-dependent activation of cAMP/PKA was shown to result from a combination of transmembrane and soluble calcium-dependent adenylyl cyclases [75]. More recently, Nicol et al. [76] described spatial and temporal features that regulate axon guidance in Xenopus spinal neurons: the cAMP/calcium interaction differ in different regions of the growth cone.

## 6 Biosensor imaging to analyze the regulation of cAMP/PKA signals

### 6.1 Phosphodiesterases degrade cAMP

Neuronal cells exhibit a complex tridimensional structure, which delimit spatial domains with specific integrative

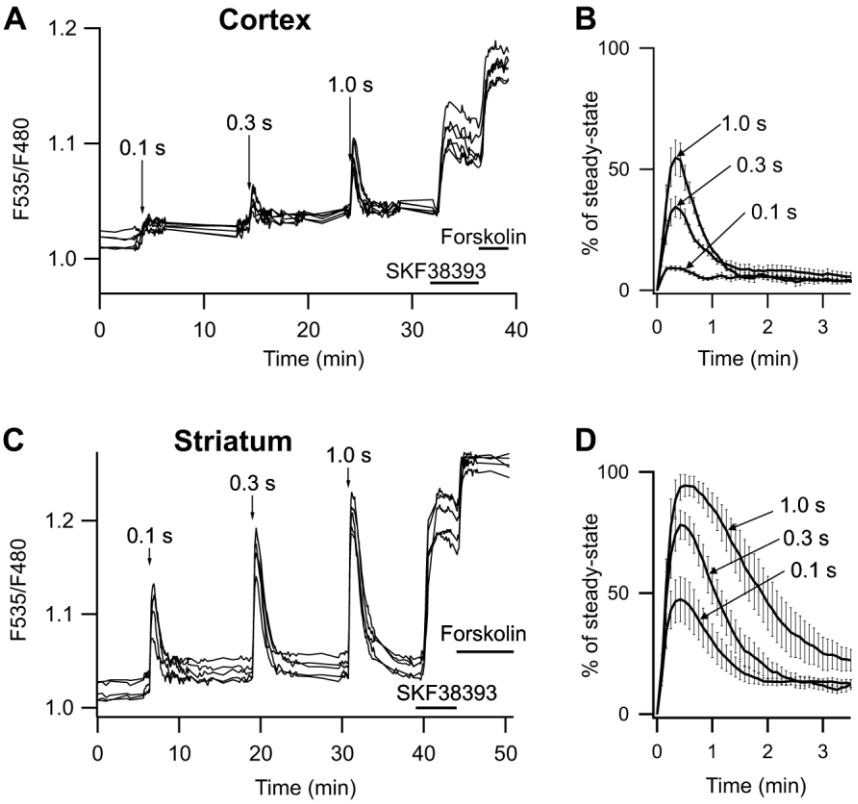


**Figure 4.** Biosensor imaging uncovers differences in response dynamics between two neuronal types: striatal neurons respond more efficiently than pyramidal cortical neurons to a brief dopaminergic stimulation. Dopamine was released transiently from a caged precursor ((N)-1-(2-Nitrophenyl)ethyl-carboxy-3 ,4-dihydroxyphenethylamine dopamine, 5 µM) by a flash of UV light. (**A**) Pyramidal cortical neurons expressing AKAR3 were imaged in wide-field microscopy and the ratio was plotted against time. Arrows indicate the UV flash, for the duration indicated on the arrow. Increases in the duration of the flash were associated with increases in the amplitude of the ratio response. (**B**) Responses were normalized with respect to the steady-state response to bath-applied SKF38393 and averaged; error bars indicate SEM; $n = 6$. (**C**, **D**) As in (A, B), except that the recording were performed in the striatum; $n = 5$. Amplitudes differed between cortex and striatum with 0.3 an 1 s uncaging times ($p<0.001$; unpaired two-tailed t tests). The figure is from [56].

properties. Many neuromodulatory signals come as discrete events, which trigger a series of intracellular activating events closely followed by feedback events eventually returning the cell to the "basal" state. These negative control mechanisms include PDE that efficiently degrade cyclic nucleotides. The 21 genes encoding for the 11 PDE families are translated into more than 50 different enzymes by alternative splicing, with unique subcellular distributions and regulatory domains. For example PC12 cells express high levels of PDE3 and biosensor imaging revealed that PDE3 is responsible of the submembrane compartmentation of the cAMP signal produced by EGF and NGF [69]. In retinal ganglion cells, calcium-stimulated cAMP/PKA signaling was shown to be regulated by calcium-stimulated PDE1 [75], further complicating the integration of coincident cAMP and calcium signals.

Recently, the use of biosensors allowed for the functional characterization of PDE4 in pyramidal neurons of the cortex [38]. In the somatic cytosol, PDE4 was shown to tightly regulate the amplitude of the cAMP responses to β-adrenergic and $D_1$-dopaminergic stimulation [38, 56]. In small dendrites, where the surface-over-volume ratio is enhanced, PDE4 controls the tonic production of cAMP by adenylyl cyclases [38]. These results demonstrate that PDE4 is a crucial regulator of adrenergic and dopaminergic responses and allow for the subcellular compartmentation of the cAMP signal in pyramidal neurons [9, 38].

Biosensor imaging also allows to study the dynamic interactions between signaling cascades. In striatal neurons, NO donors increase intracellular cGMP concentration, which activates PDE2 and therefore inhibits the cAMP/PKA signal. This was shown by analyzing the time-course of transient cAMP responses to brief forskolin applications: these cAMP transients where smaller in amplitude and shorter in duration when PDE2 was activated by cGMP [43].

### 6.2 Phosphatases dephosphorylate PKA substrates

The time-course of the AKAR response is determined by different factors including cAMP accumulation and PKA phosphorylation rate. The role exerted by phosphatases in the rate of dephosphorylation was observed experimentally in brain slices where adenylyl cyclase were activated in the presence of phosphatase inhibitors: in these conditions, adenylyl cyclase stimulation led to an increase in AKAR phosphorylation that barely recovered after the agonist removal [70]. Thus, one can assume that the phosphorylation level of the biosensor results from the equilibrium between PKA-dependent phosphorylation and dephosphorylation performed by phosphatases.

In striatal neurons, protein phosphatase 1 (PP1) is strongly inhibited by DARPP-32 when its threonine 34 residue is phosphorylated by PKA [77]. Using a knock-in mutant mouse, in which the threonine residue was

replaced with an alanine (DARPP-32-T34A) [78], the authors evaluated the PKA response to brief dopamine receptor stimulation: in the mutant mouse, neither the kinetics of increase nor the amplitude of the transient PKA response were modified; however, the rate of the decay was much faster, consistent with a lack of phosphatase inhibition. These results show that, by inhibiting phosphatase 1, DARPP-32 exerts a strong positive feedback regulation on PKA signaling, by maintaining PKA targets in their phosphorylated state.

## 7 Conclusions

During the last decade, the incredible power of genetics have uncovered the involvement of a number of genes in various neuropsychiatric diseases, while medicinal chemistry has created highly specific drugs for a number of signaling enzymes. Many times however, the precise function of these signaling enzymes remains mysterious. Biosensor imaging, by providing a dynamic picture of signaling processes tremendously help understand the fundamentals of integrative processes taking place in living and individual neurons. We believe that this type of approach can be instrumental in understanding the mechanism of action of a number of drugs at the preclinical level. In addition, while cAMP/PKA biosensor imaging in vivo has only been performed on Drosophila so far [67, 68], calcium imaging in the brain of living rodents is routinely performed and no technological obstacle precludes real-time analysis of cAMP/PKA processes in the brain of a living animal. This would indeed open considerable perspectives for both fundamental and preclinical research.

*This work was supported by Centre National de la Recherche Scientifique, UPMC, the École des Neurosciences de Paris Ile-de-France and Labex BioPsy.*

*The authors declare no conflict of interest.*

## 8 References

[1] Craven, K. B., Zagotta, W. N., CNG and HCN channels: Two peas, one pod. *Annu. Rev. Physiol.* 2006, *68*, 375–401.
[2] Kaupp, U. B., Seifert, R., Molecular diversity of pacemaker ion channels. *Annu. Rev. Physiol.* 2001, *63*, 235–257.
[3] Gloerich, M., Bos, J. L., Epac: Defining a new mechanism for cAMP action. *Annu. Rev. Pharmacol. Toxicol.* 2010, *50*, 355–375.
[4] Tasken, K., Aandahl, E. M., Localized effects of cAMP mediated by distinct routes of protein kinase A. *Physiol. Rev.* 2004, *84*, 137–167.
[5] Taylor, S. S., Buechler, J. A., Yonemoto, W., cAMP-dependent protein kinase: Framework for a diverse family of regulatory enzymes. *Annu. Rev. Biochem.* 1990, *59*, 971–1005.
[6] Taylor, S. S., Ilouz, R., Zhang, P., Kornev, A. P., Assembly of allosteric macromolecular switches: Lessons from PKA. *Nat. Rev. Mol. Cell Biol.* 2012, *13*, 646–658.
[7] Bockaert, J., Perroy, J., Becamel, C., Marin, P. et al., GPCR interacting proteins (GIPs) in the nervous system: Roles in physiology and pathologies. *Annu. Rev. Pharmacol. Toxicol.* 2010, *50*, 89–109.
[8] Scott, J. D., Dessauer, C. W., Tasken, K., Creating order from chaos: Cellular regulation by kinase anchoring. *Annu. Rev. Pharmacol. Toxicol.* 2013, *53*, 187–210.
[9] Neves, S. R., Tsokas, P., Sarkar, A., Grace, E. A. et al., Cell shape and negative links in regulatory motifs together control spatial information flow in signaling networks. *Cell* 2008, *133*, 666–680.
[10] Zhang, J., Campbell, R. E., Ting, A. Y., Tsien, R. Y., Creating new fluorescent probes for cell biology. *Nat. Rev. Mol. Cell Biol.* 2002, *3*, 906–918.
[11] Miyawaki, A., Visualization of the spatial and temporal dynamics of intracellular signaling. *Dev. Cell* 2003, *4*, 295–305.
[12] Knopfel, T., Genetically encoded optical indicators for the analysis of neuronal circuits. *Nat. Rev. Neurosci.* 2012, *13*, 687–700.
[13] Looger, L. L., Griesbeck, O., Genetically encoded neural activity indicators. *Curr. Opin. Neurobiol.* 2011, *22*, 18–23.
[14] Okumoto, S., Looger, L. L., Micheva, K. D., Reimer, R. J. et al., Detection of glutamate release from neurons by genetically encoded surface-displayed FRET nanosensors. *Proc. Natl. Acad. Sci. USA* 2005, *102*, 8740–8745.
[15] Hires, S. A., Zhu, Y., Tsien, R. Y., Optical measurement of synaptic glutamate spillover and reuptake by linker optimized glutamate-sensitive fluorescent reporters. *Proc. Natl. Acad. Sci. USA* 2008, *105*, 4411–4416.
[16] Dulla, C., Tani, H., Okumoto, S., Frommer, W. B. et al., Imaging of glutamate in brain slices using FRET sensors. *J. Neurosci. Methods* 2008, *168*, 306–319.
[17] Marvin, J. S., Borghuis, B. G., Tian, L., Cichon, J. et al., An optimized fluorescent probe for visualizing glutamate neurotransmission. *Nat. Methods* 2013, *10*, 162–170.
[18] Rich, T. C., Tse, T. E., Rohan, J. G., Schaack, J. et al., In vivo assessment of local phosphodiesterase activity using tailored cyclic nucleotide-gated channels as cAMP sensors. *J. Gen. Physiol.* 2001, *118*, 63–78.
[19] Rich, T. C., Fagan, K. A., Tse, T. E., Schaack, J. et al., A uniform extracellular stimulus triggers distinct cAMP signals in different com-

**Pierre Vincent** started his scientific career studying neurotransmission in the brain using electrophysiological approaches. Together with Roger Y. Tsien, he developed real-time imaging of cAMP signals in neurons. He is now leading a research team in Paris which routinely uses genetically-encoded biosensors expressed in rodent brain slices to study the spatial and temporal properties of the cyclic nucleotide signaling cascade. The team has a particular interest in the functional role played by phosphodiesterases and phosphatases in determining the integrative properties of neurons. Current work focuses on the mechanism of action of drugs which target neuropsychiatric diseases.

partments of a simple cell. *Proc. Natl. Acad. Sci. USA* 2001, *98*, 13049–13054.
[20] Wouters, F. S., Verveer, P. J., Bastiaens, P. I., Imaging biochemistry inside cells. *Trends Cell Biol.* 2001, *11*, 203–211.
[21] Jares-Erijman, E. A., Jovin, T. M., FRET imaging. *Nat. Biotechnol.* 2003, *21*, 1387–1395.
[22] Umezawa, Y., Genetically encoded optical probes for imaging cellular signaling pathways. *Biosens. Bioelectron.* 2005, *20*, 2504–2511.
[23] Adams, S. R., Harootunian, A. T., Buechler, Y. J., Taylor, S. S. et al., Fluorescence ratio imaging of cyclic AMP in single cells. *Nature* 1991, *349*, 694–697.
[24] Bacskai, B. J., Hochner, B., Mahaut-Smith, M., Adams, S. R. et al., Spatially resolved dynamics of cAMP and protein kinase A subunits in Aplysia sensory neurons. *Science* 1993, *260*, 222–226.
[25] Hempel, C. M., Vincent, P., Adams, S. R., Tsien, R. Y. et al., Spatio-temporal dynamics of cyclic AMP signals in an intact neural circuitm. *Nature* 1996, *384*, 166–169.
[26] Gorbunova, Y. V., Spitzer, N. C., Dynamic interactions of cyclic AMP transients and spontaneous Ca(2+) spikes. *Nature* 2002, *418*, 93–96.
[27] Vincent, P., Brusciano, D., Cyclic AMP imaging in neurones in brain slice preparations. *J. Neurosci. Methods* 2001, *108*, 189–198.
[28] Goaillard, J. M., Vincent, P., Serotonin suppresses the slow afterhyperpolarization in rat intralaminar and midline thalamic neurones by activating 5-HT(7) receptors. *J. Physiol.* 2002, *541*, 453–465.
[29] Zaccolo, M., De Giorgi, F., Cho, C. Y., Feng, L. et al., A genetically encoded, fluorescent indicator for cyclic AMP in living cells. *Nat. Cell Biol.* 2000, *2*, 25–29.
[30] Lissandron, V., Terrin, A., Collini, M., D'alfonso, L. et al., Improvement of a FRET-based indicator for cAMP by linker design and stabilization of donor–acceptor interaction. *J. Mol. Biol.* 2005, *354*, 546–555.
[31] Zaccolo, M., Di Benedetto, G., Lissandron, V., Mancuso, L. et al., Restricted diffusion of a freely diffusible second messenger: Mechanisms underlying compartmentalized cAMP signalling. *Biochem. Soc. Trans.* 2006, *34*, 495–497.
[32] Di Benedetto, G., Zoccarato, A., Lissandron, V., Terrin, A. et al., Protein kinase A type I and type II define distinct intracellular signaling compartments. *Circ. Res.* 2008, *103*, 836–844.
[33] Nikolaev, V. O., Bunemann, M., Hein, L., Hannawacker, A. et al., Novel single chain cAMP sensors for receptor-induced signal propagation. *J. Biol. Chem.* 2004, *279*, 37215–37218.
[34] DiPilato, L. M., Cheng, X., Zhang, J., Fluorescent indicators of cAMP and Epac activation reveal differential dynamics of cAMP signaling within discrete subcellular compartments. *Proc. Natl. Acad. Sci. USA* 2004, *101*, 16513–16518.
[35] Ponsioen, B., Zhao, J., Riedl, J., Zwartkruis, F. et al., Detecting cAMP-induced Epac activation by fluorescence resonance energy transfer: Epac as a novel cAMP indicator. *EMBO Rep.* 2004, *5*, 1176–1180.
[36] Calebiro, D., Nikolaev, V. O., Gagliani, M. C., de Filippis, T. et al., Persistent cAMP-signals triggered by internalized G-protein-coupled receptors. *PLoS Biol.* 2009, *7*, e1000172.
[37] Norris, R. P., Ratzan, W. J., Freudzon, M., Mehlmann, L. M. et al., Cyclic GMP from the surrounding somatic cells regulates cyclic AMP and meiosis in the mouse oocyte. *Development* 2009, *136*, 1869–1878.
[38] Castro, L. R., Gervasi, N., Guiot, E., Cavellini, L. et al., Type 4 phosphodiesterase plays different integrating roles in different cellular domains in pyramidal cortical neurons. *J. Neurosci.* 2010, *30*, 6143–6151.
[39] Nikolaev, V. O., Bunemann, M., Schmitteckert, E., Lohse, M. J. et al., Cyclic AMP imaging in adult cardiac myocytes reveals far-reaching β1-adrenergic but locally confined β2-adrenergic receptor-mediated signaling. *Circ. Res.* 2006, *99*, 1084–1091.
[40] van der Krogt, G. N., Ogink, J., Ponsioen, B., Jalink, K., A comparison of donor–acceptor pairs for genetically encoded FRET sensors: Application to the Epac cAMP sensor as an example. *PLoS ONE* 2008, *3*, e1916.
[41] Hong, K. P., Spitzer, N. C., Nicol, X., Improved molecular toolkit for cAMP studies in live cells. *BMC Res. Notes* 2011, *4*, 241.
[42] Klarenbeek, J. B., Goedhart, J., Hink, M. A., Gadella, T. W. et al., A mTurquoise-based cAMP sensor for both FLIM and ratiometric read-out has improved dynamic range. *PLoS ONE* 2011, *6*, e19170.
[43] Polito, M., Klarenbeek, J., Jalink, K., Paupardin-Tritsch, D. et al., The NO/cGMP pathway inhibits transient cAMP signals through the activation of PDE2 in striatal neurons. *Front. Cell. Neurosci.* 2013, *7*, 211.
[44] Zhang, J., Ma, Y., Taylor, S. S., Tsien, R. Y., Genetically encoded reporters of protein kinase A activity reveal impact of substrate tethering. *Proc. Natl. Acad. Sci. USA* 2001, *98*, 14997–15002.
[45] Zhang, J., Hupfeld, C. J., Taylor, S. S., Olefsky, J. M. et al., Insulin disrupts beta-adrenergic signalling to protein kinase A in adipocytes. *Nature* 2005, *437*, 569–573.
[46] Allen, M. D., Zhang, J., Subcellular dynamics of protein kinase A activity visualized by FRET-based reporters. *Biochem. Biophys. Res. Commun.* 2006, *348*, 716–721.
[47] Depry, C., Allen, M. D., Zhang, J., Visualization of PKA activity in plasma membrane microdomains. *Mol. Biosyst.* 2011, *7*, 52–58.
[48] Erard, M., Fredj, A., Pasquier, H., Beltolngar, D. B. et al., Minimum set of mutations needed to optimize cyan fluorescent proteins for live cell imaging. *Mol. Biosyst.* 2013, *9*, 258–267.
[49] Friedrich, M. W., Aramuni, G., Mank, M., Mackinnon, J. A. et al., Imaging CREB activation in living cells. *J. Biol. Chem.* 2010, *285*, 23285–23295.
[50] Leroy, J., Abi-Gerges, A., Nikolaev, V. O., Richter, W. et al., Spatiotemporal dynamics of beta-adrenergic cAMP signals and L-type Ca2+ channel regulation in adult rat ventricular myocytes: Role of phosphodiesterases. *Circ. Res.* 2008, *102*, 1091–1100.
[51] Landa, L. R. J., Harbeck, M., Kaihara, K., Chepurny, O. et al., Interplay of Ca2+ and cAMP signaling in the insulin-secreting MIN6 beta-cell line. *J. Biol. Chem.* 2005, *280*, 31294–31302.
[52] Violin, J. D., Dipilato, L. M., Yildirim, N., Elston, T. C. et al., β2-Adrenergic receptor signaling and desensitization elucidated by quantitative modeling of real time cAMP dynamics. *J. Biol. Chem.* 2008, *283*, 2949–2961.
[53] Dunn, T. A., Wang, C. T., Colicos, M. A., Zaccolo, M. et al., Imaging of cAMP levels and protein kinase a activity reveals that retinal waves drive oscillations in second-messenger cascades. *J. Neurosci.* 2006, *26*, 12807–12815.
[54] Mironov, S. L., Skorova, E., Taschenberger, G., Hartelt, N. et al., Imaging cytoplasmic cAMP in mouse brainstem neurons. *BMC Neurosci.* 2009, *10*, 29.
[55] Hu, E., Demmou, L., Cauli, B., Gallopin, T. et al., VIP, CRF, and PACAP act at distinct receptors to elicit different cAMP/PKA dynamics in the neocortex. *Cereb. Cortex* 2011, *21*, 708–718.
[56] Castro, L. R., Brito, M., Guiot, E., Polito, M. et al., Striatal neurones have a specific ability to respond to phasic dopamine release. *J. Physiol.* 2013, *591*, 3197–3214.
[57] Dunn, T. A., Feller, M. B., Imaging second messenger dynamics in developing neural circuits. *Dev. Neurobiol.* 2008, *68*, 835–844.
[58] Shelly, M., Lim, B. K., Cancedda, L., Heilshorn, S. C. et al., Local and long-range reciprocal regulation of cAMP and cGMP in axon/dendrite formation. *Science* 2010, *327*, 547–552.
[59] Grynkiewicz, G., Poenie, M., Tsien, R. Y., A new generation of Ca2+ indicators with greatly improved fluorescence properties. *J. Biol. Chem.* 1985, *260*, 3440–3450.
[60] Börner, S., Schwede, F., Schlipp, A., Berisha, F. et al., FRET measurements of intracellular cAMP concentrations and cAMP analog permeability in intact cells. *Nat. Protoc.* 2011, *6*, 427–438.

[61] van der Wal, J., Habets, R., Varnai, P., Balla, T. et al., Monitoring agonist-induced phospholipase C activation in live cells by fluorescence resonance energy transfer. *J. Biol. Chem*. 2001, *276*, 15337–15344.
[62] Drobac, E., Tricoire, L., Chaffotte, A.F., Guiot, E. et al., Calcium imaging in single neurons from brain slices using bioluminescent reporters. *J. Neurosci. Res*. 2010, *88*, 695–711.
[63] Shafer, O. T., Kim, D. J., Dunbar-Yaffe, R., Nikolaev, V. O. et al., Widespread receptivity to neuropeptide PDF throughout the neuronal circadian clock network of Drosophila revealed by real-time cyclic AMP imaging. *Neuron* 2008, *58*, 223–237.
[64] Duvall, L. B., Taghert, P. H., The circadian neuropeptide PDF signals preferentially through a specific adenylate cyclase isoform AC3 in M pacemakers of Drosophila. *PLoS Biol*. 2012, *10*, e1001337.
[65] Bateup, H. S., Svenningsson, P., Kuroiwa, M., Gong, S. et al., Cell type-specific regulation of DARPP-32 phosphorylation by psychostimulant and antipsychotic drugs. *Nat. Neurosci*. 2008, *11*, 932–939.
[66] Bertran-Gonzalez, J., Bosch, C., Maroteaux, M., Matamales, M. et al., Opposing patterns of signaling activation in dopamine D1 and D2 receptor-expressing striatal neurons in response to cocaine and haloperidol. *J. Neurosci*. 2008, *28*, 5671–5685.
[67] Tomchik, S. M., Davis, R. L., Dynamics of learning-related cAMP signaling and stimulus integration in the Drosophila olfactory pathway. *Neuron* 2009, *64*, 510–521.
[68] Gervasi, N., Tchenio, P., Preat, T., PKA dynamics in a Drosophila learning center: Coincidence detection by rutabaga adenylyl cyclase and spatial regulation by dunce phosphodiesterase. *Neuron* 2010, *65*, 516–529.
[69] Herbst, K. J., Allen, M. D., Zhang, J., Spatiotemporally regulated PKA activity is a critical regulator of growth factor-stimulated ERK signaling in PC12 cells. *Mol. Cell Biol*. 2011, *31*, 4063–4075.
[70] Gervasi, N., Hepp, R., Tricoire, L., Zhang, J. et al., Dynamics of protein kinase A signaling at the membrane, in the cytosol, and in the nucleus of neurons in mouse brain slices. *J. Neurosci*. 2007, *27*, 2744–2750.
[71] Wachten, S., Masada, N., Ayling, L. J., Ciruela, A. et al., Distinct pools of cAMP centre on different isoforms of adenylyl cyclase in pituitary-derived GH3B6 cells. *J. Cell Sci*. 2010, *123*, 95–106.
[72] Saucerman, J. J., Zhang, J., Martin, J. C., Peng, L. X. et al., Systems analysis of PKA-mediated phosphorylation gradients in live cardiac myocytes. *Proc. Natl. Acad. Sci. USA* 2006, *19*, 2650–2658.
[73] Harbeck, M. C., Chepurny, O., Nikolaev, V. O., Lohse, M. J. et al., Simultaneous optical measurements of cytosolic Ca2+ and cAMP in single cells. *Sci. STKE* 2006, *2006*, pl6.
[74] Willoughby, D., Cooper, D. M., Ca2+ stimulation of adenylyl cyclase generates dynamic oscillations in cyclic AMP. *J. Cell Sci*. 2006, *119*, 828–836.
[75] Dunn, T. A., Storm, D. R., Feller, M. B., Calcium-dependent increases in protein kinase-A activity in mouse retinal ganglion cells are mediated by multiple adenylate cyclases. *PLoS ONE* 2009, *4*, e7877.
[76] Nicol, X., Hong, K. P., Spitzer, N. C., Spatial and temporal second messenger codes for growth cone turning. *Proc. Natl. Acad. Sci. USA* 2011, *108*, 13776–13781.
[77] Svenningsson, P., Nishi, A., Fisone, G., Girault, J. A. et al., DARPP-32: An integrator of neurotransmission. *Annu. Rev. Pharmacol. Toxicol*. 2004, *44*, 269–296.
[78] Svenningsson, P., Tzavara, E. T., Carruthers, R., Rachleff, I. et al., Diverse psychotomimetics act through a common signaling pathway. *Science* 2003, *302*, 1412–1415.
[79] Polito, M., Vincent, P., Guiot, E., Biosensor imaging in brain slice preparations. in: Zhang, J. et al. (Eds.), *Fluorescent protein-based biosensors: Methods and protocols, methods in molecular biology*, Vol. 1071, Humana Press 2014, pp. 175–194.

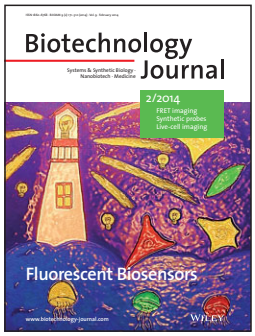


The Fluorescent Biosensor special issue of *Biotechnology Journal* is edited by Dr. May Morris and Prof. Marc Blondel. The cover image is an artistic interpretation of how fluorescent biosensors function as molecular beacons for scientists navigating a sea of molecules. Image courtesy of L. Divita and R. Wintergerst.

## *Biotechnology Journal* – list of articles published in the February 2014 issue.